Article

Comparative Reliability Assessment of Hybrid Si/SiC and Conventional Si Power Module Based PV Inverter Considering Mission Profile of India and Denmark Locations

Sainadh Singh Kshatri [1], **Javed Dhillon** [2], **Sachin Mishra** [2], **Ali Torabi Haghighi** [3], **Julian David Hunt** [4] and **Epari Ritesh Patro** [3,*]

1   Department of Electrical and Electronics Engineering, B V Raju Institute of Technology, Narsapur 502313, Telangana, India
2   School of Electronics and Electrical Engineering, Lovely Professional University, Phagwara 144411, Punjab, India
3   Water, Energy, and Environmental Engineering Research Unit, University of Oulu, P.O. Box 4300, FIN-90014 Oulu, Finland
4   International Institute for Applied Systems Analysis (IIASA), Schlossplatz 1, A-2361 Laxenburg, Austria
*   Correspondence: ritesh.patro@oulu.fi

Abstract: Energy harnessing from renewable energy sources has become more flexible with power electronic technologies. Recent advancements in power electronic technologies achieve converter efficiency higher than 98%. Today, reliable power electronic devices are needed to design a PV-based energy converter (inverter) to reduce the risk of failure and maintenance costs during operation. Wide-bandgap SiC devices are becoming more common in power electronic converters. These devices are designed to reduce switching loss and improve the efficiency of the system. Nevertheless, the cost of SiC devices is a major concern. Hence, to improve the reliability of the PV inverter while considering the economic aspects, this paper develops a highly reliable PV inverter with a hybrid Si/SiC power module that consists of a Si-IGBT with a SiC anti-parallel diode. A test case of a 3 kW PV inverter is considered for reliability analysis. The loading of the PV inverter is done under uncertain environmental conditions by considering the yearly Mission Profile (MP) data related to Ambient Temperature (AT) and Solar Irradiance (SI) at the India and Denmark locations. The effectiveness of the proposed hybrid Si/SiC power module is tested by comparing it with a conventional IGBT power module. The results showcase the marked improvement in PV inverter reliability with the proposed hybrid power module.

Keywords: mission profile; Si/SiC-IGBT; Photovoltaic (PV) Inverter; Junction Temperature (T_j)

1. Introduction

The use of renewable energy sources has increased the demand for power electronics devices for energy conversion in the last decade. In renewable energy systems, power electronic converters share about 59% of the total cost. A survey in [1,2] shows that power electronic converters are the most unreliable components. According to [3], thermal stress is the critical stressor of power semiconductors and leads to failure. Solder-die fatigue and bond wire lift-off are the two most common failures in power semiconductors. Hence, the reliability of power electronics is a serious concern and needs to be modified to reduce the risk of failure and maintenance costs during operation. Today, PV energy conversion systems (i.e., inverters) require power electronics devices with low failure rates to provide high reliability.

Conventional Si-based power electronics switches have reached their theoretical limits and are not capable of addressing current power needs. Significant advancements are made in Si-IGBTs, but in the case of Si diodes, these advancements are not up to the mark

and restrict the performance of power electronic converters [4]. In [5], SiC-based power electronic switches are provided with a wide bandgap that performs superiorly compared to conventional Si-based devices. The notable advantages of SiC-based devices are low switching losses, high switching speed, blocking voltage, etc. Hence, the performance of the system will improve. Nevertheless, the cost of SiC devices is a major concern. Hence, it is not economical to replace all the devices in the PV inverter with SiC devices. To overcome this issue, hybrid applications of Si/SiC based devices have been proposed in many studies [6–12].

An active gate-controlled technique is designed in [7] to improve the efficiency of the hybrid Si/SiC-based inverter. The design of a hybrid module with Si-IGBT and SiC MOSFET is discussed in [8]. In [9], the application of a hybrid module, i.e., Si/SBD, for the current source ZCSI based on a DC-DC converter has been presented. To reduce converter losses in [13], a model with a TJ controller was used. In [14], the author proposed the design of a hybrid, three-level NPC inverter. It consists of four Si-IGBTs and two SiC MOSFETs for reliability improvement. Additionally, the authors addressed the cost limit constraint of SiC-based devices. The application of a hybrid Si/SiC power module in a half bridge-traction inverter is presented in [15]. A comparative study between Si and SiC-based devices for ANPC inverters is presented in [16]. Performance comparison studies of the DC-DC converter in electric vehicles are presented in [10], considering hybrid Si/SiC power modules. In [17], the authors presented an optimal gate control for T_j balance and power loss minimization considering hybrid Si/SiC power modules. Related work is also presented in [18–22]. In [23], the authors presented the experimental validation of hybrid supercapacitors and battery-based renewable energy systems. Standalone inverter experimental validation for hybrid PV and wind systems is presented in [24]. Still, there is a gap in the reliability analysis of hybrid Si/SiC power modules needed to design a highly reliable inverter.

To improve the reliability of the PV inverter considering the economic aspects, this paper proposes a highly reliable PV inverter with a hybrid Si/SiC power module that consists of Si-IGBT with SiC Schottky anti-parallel diodes. The cost of the SiC material is very high, and it is not economical to use SiC-IGBT. As a result, SiC is used for diodes because it absorbs the majority of the diode's losses. A test case of a 3 kW PV inverter for grid-connected applications is considered for reliability analysis. The loading of a PV inverter under uncertain environmental conditions, i.e., MP (AT, SI), impacts its reliability; hence, yearly MP at India [25] and Denmark [26] locations are considered during reliability analysis. The effectiveness of the proposed hybrid Si/SiC power module is tested by comparing it with a conventional IGBT power module. The results showcase the marked improvement in PV inverter reliability with the proposed hybrid power module.

2. Reliability Analysis of Hybrid Si/SiC Module Based PV Inverter

The flow chart for reliability analysis of a hybrid Si/SiC module-based PV inverter is shown in Figure 1.
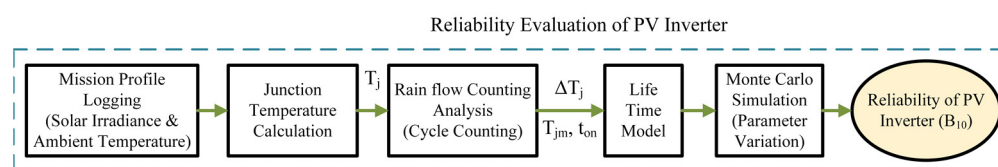
Reliability Evaluation of PV Inverter

Figure 1. Flow chart for reliability analysis.

For the MP-oriented reliability analysis, real-time SI and AI data (1-minute resolution for 1 year) from various locations must be logged. Annual MP at the India and Denmark locations are considered in this paper and shown in Figure 2a,b, respectively.
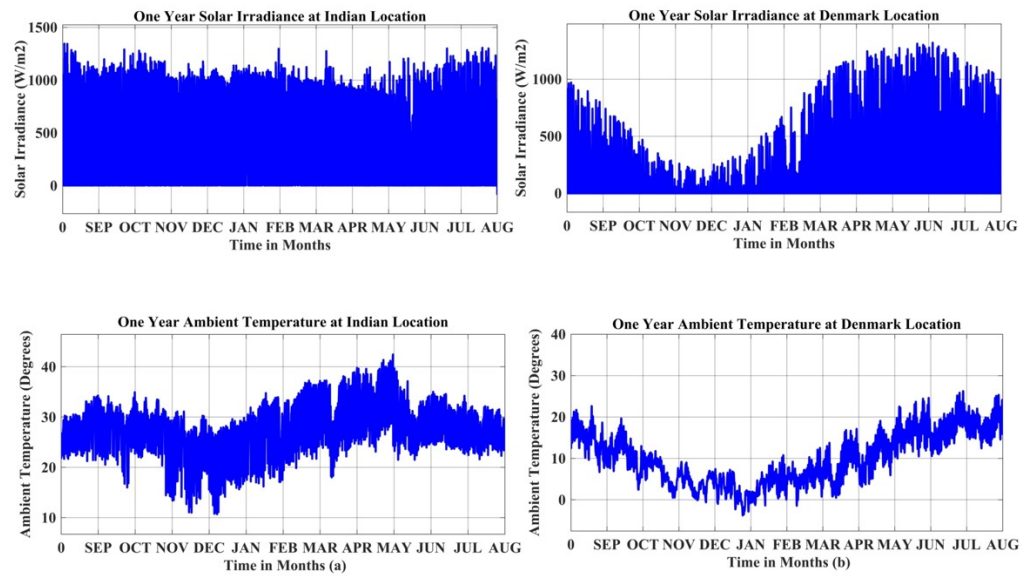
Figure 2. (**a**) Yearly MP data in the India location; (**b**) Yearly MP data in the Denmark location.

From the yearly MP shown in Figure 2, Junction Temperature (T_j) needs to be calculated. Nevertheless, T_j cannot be measured directly from the hybrid Si/SiC power module; hence, an indirect method, i.e., the foster electro-thermal model (FETM), is used in this paper as shown in Figure 3.
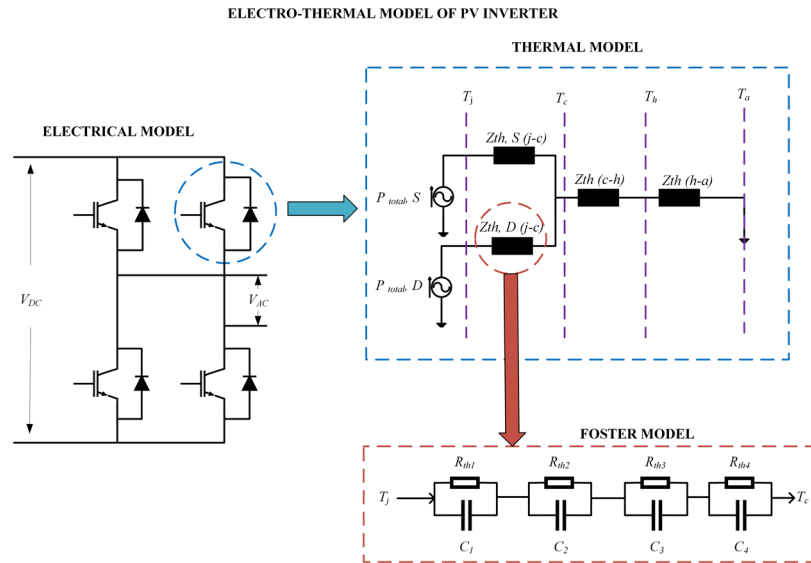

Figure 3. FETM of a PV inverter.

The mathematical expression of T_j is calculated by Equation (1) below.

$$T_j = Z_{th\,(j-c)} * P_T + T_C \tag{1}$$

where $Z_{th(j-c)}$ is the impedance between the junction and the case, P_T is the total loss of power, and T_c is the temperature of the case.

From the yearly T_j, N_i, T_{jm}, and ΔT_j, which are obtained using the rainflow-counting algorithm [27]. The lifetime can be calculated using Miner's rule, as shown in Equation (2).

$$LT = \frac{1}{LC} \tag{2}$$

where LC is the life consumption and is expressed as:

$$LC = \sum \frac{n_i}{K(\Delta T_j)^{\beta_1} . e^{\frac{\beta_2}{(T_j + 273K)}} . t_{on}^{\beta_3} . I^{\beta_4} . V^{\beta_5} . D^{\beta_6}} \tag{3}$$

The parameters in LC are considered from the Bayerer's lifetime model [26] and tabulated in Table 1.

Table 1. Parameters of the lifetime equation.

Name	Number
Factor (A)	9.340×10^{14}
β_1	-4.42
β_2	1285.00
β_3	-0.46
β_4	-0.72
β_5	-0.76
β_6	-0.50
Foot Bond Current (*I*)	3–23 A
Class of Voltage (*V*)	6–33 V
Diameter	75–500 μm

In the above lifetime model, all the parameters are constant, i.e., all the devices should fail at the same rate, but practically this is not feasible, so to overcome this, a variation of 5% is implemented. A Monte Carlo simulation is used to generate 10,000 samples. All the generated lifetimes are distributed in the Weibull distribution to obtain the reliability function as given in Equation (4):

$$R_i(t) = e^{-\left(\frac{t}{\alpha}\right)^{\gamma}} \tag{4}$$

where:

α is the scale parameter;

γ is the shape parameter.

In Equation (4), the shape parameter γ is obtained from the Weibull distribution, and the scale parameter α is the characteristic lifetime where 63.2% of the population has failed [28]. The above reliability function is used to calculate the component and SL reliability as defined in Equation (5):

$$R_{total}(t) = \prod_{i=1}^{n} R_i(t) \tag{5}$$

where $R_i(t)$ is the individual component reliability.

The B_{10} lifetime can be calculated using Equation (6):

$$B_x = \left[\ln\left(\frac{100}{100 - x}\right) \times (\alpha)^{\gamma} \right]^{\frac{1}{\gamma}} \tag{6}$$

where:

x is the percentage of the population;

α is the scale parameter;

γ is the shape parameter.

3. Results and Discussions

In this paper, a test case of a 3 kW PV inverter for a grid-connected application is considered for the reliability analysis, as shown in Figure 4. A PV inverter consists of four 600 V/30 A hybrid switches (Si-IGBT (IGW30N60H3) or SiC-Schottky diodes (C3D20060D)) as shown in Figure 5. Its effectiveness is analyzed by comparing it to a conventional switch (Si-IGBT (IGW30N60H3) or Si-Schottky diode (IGW30N60H3)).
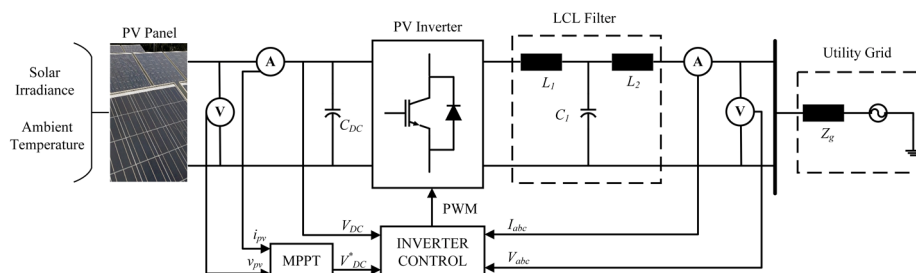

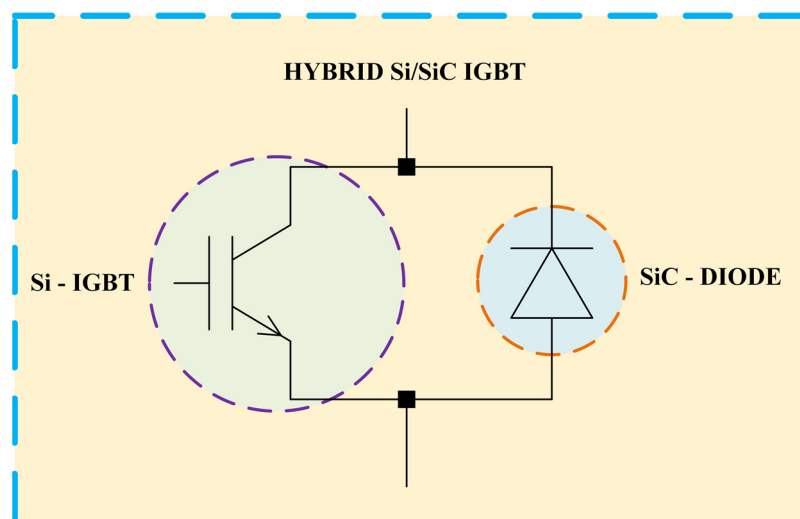**Figure 4.** A 3 kW grid-connected PV inverter.

Figure 5. Hybrid IGBT.

The specifications for this test case are taken from the research in [23].
In this paper, the following cases are considered for evaluation:

- Reliability-oriented performance evaluation of a PV inverter at the India location;
- Reliability-oriented performance evaluation of a PV inverter at the Denmark location.

3.1. Reliability-Oriented Performance Evaluation of a PV Inverter at the India Location

In this case, the reliability evaluation of the PV inverter is performed considering the MP data at the India location. During the reliability evaluation, a hybrid Si/SiC switch is used in the PV inverter, and its effectiveness is analyzed by comparing it with a conventional Si switch.

3.1.1. Calculation of T_j

The T_j of the proposed hybrid Si/SiC power module and conventional Si power module are calculated for yearly MP using FETM, as shown in Figure 6. From Figure 6, it is observed that overall, T_j is decreased with the proposed hybrid Si/SiC power module. The maximum and minimum T_j values recorded for the proposed hybrid Si/SiC power module are 99.33 °C and 11.39 °C, respectively. Similarly, the conventional Si power module values are 103.88 °C and 11.41 °C, respectively.
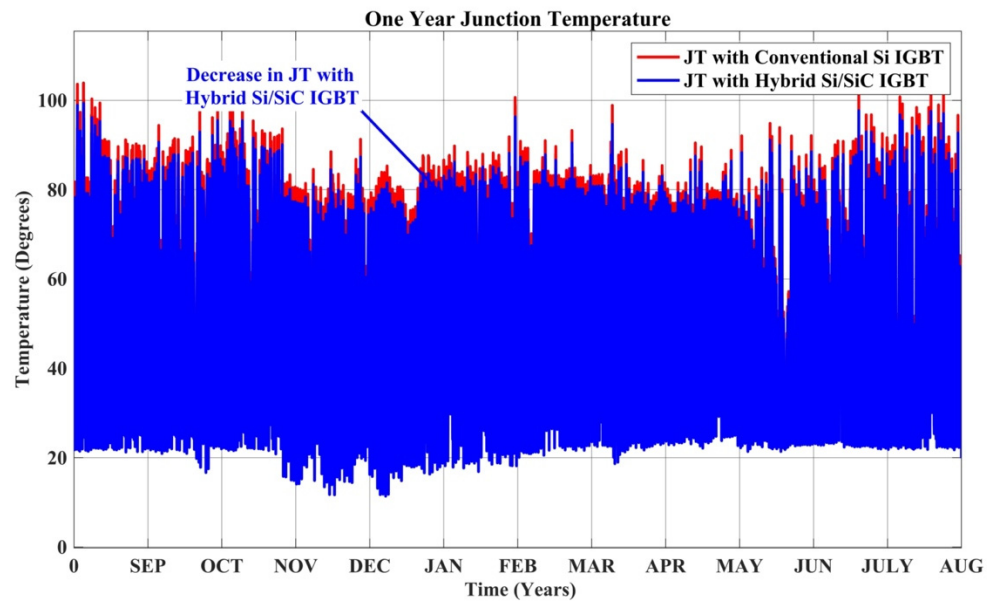
Figure 6. Yearly T_j in India.

3.1.2. Rainflow-Counting Algorithm

The T_j variations for the proposed hybrid Si/SiC power module and conventional Si power module are analyzed using the RF algorithm. The parameters N_i, T_{jm}, and ΔT_j, from T_j are obtained using the rainflow-counting algorithm.

A T_j variations histogram, i.e., N_i, T_{jm}, and ΔT for a proposed hybrid Si/SiC power module and conventional Si power module, are plotted in Figure 7. The T_{jm}, i.e., 55.66 °C, is recorded for a hybrid Si/SiC power module. Similarly, 53.9 °C is recorded for a conventional Si power module, as shown in Figure 8.
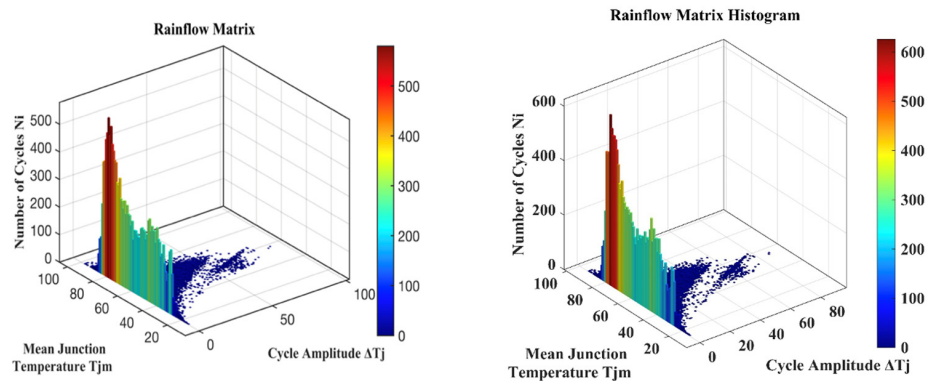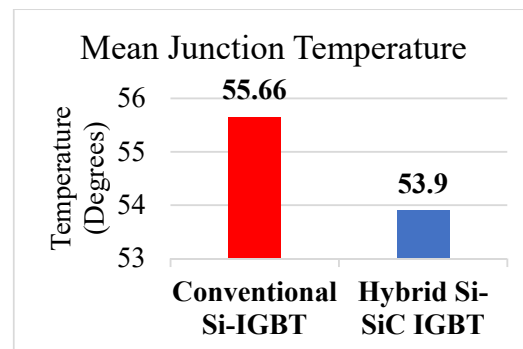

Figure 7. RF Matrix in India.

Figure 8. Mean T_j comparison.

A T$_{jm}$ of 1.76 °C is lower with the proposed hybrid Si/SiC power module.

3.1.3. MCS-Based B$_{10}$ Lifetime Evaluation

In this paper, a Monte Carlo simulation is used to generate 10,000 samples with a 5% variation, and LT is calculated at each sample using Equation (2). All the generated life times are distributed in a Weibull distribution to obtain the reliability function, as shown in Figure 9.
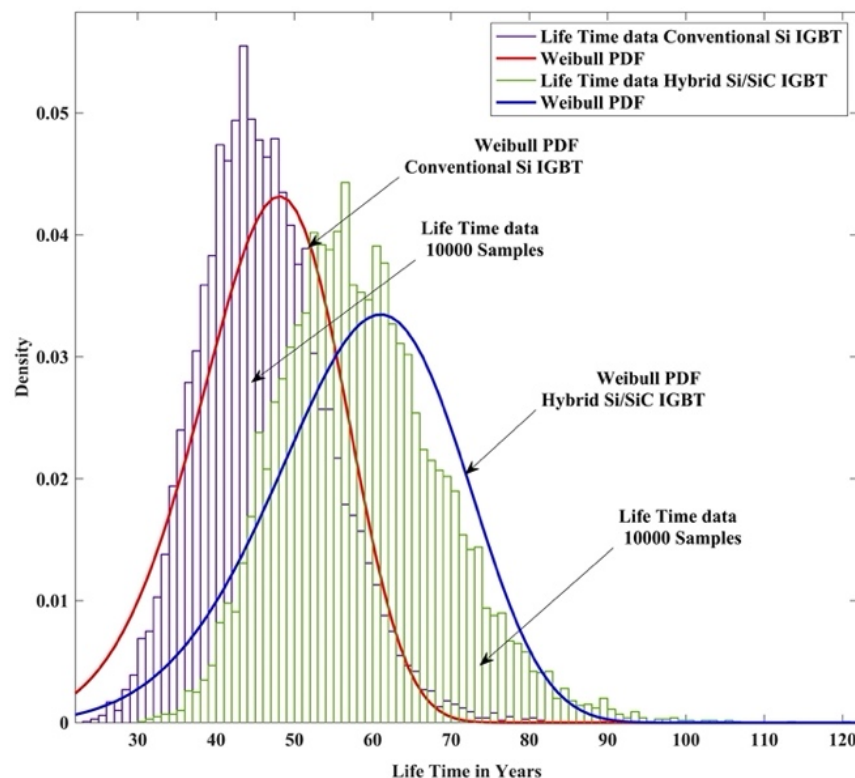

Figure 9. Lifetime distribution.

The reliability of a PV inverter is evaluated for a proposed hybrid Si/SiC power module and a conventional Si power module at both the CL and the SL using Equations (4) and (5). A B$_{10}$ lifetime is calculated using Equation (6) as shown in Figure 10. For a conventional Si-IGBT, a scale parameter, $\propto$, is 49.72 and a shape parameter, γ, is 5.74. Similarly, for a hybrid Si/SiC-IGBT scale parameter, a scale parameter, $\propto$, is 63.15, and a shape parameter, γ, is 5.65.

The B$_{10}$ lifetime at the Indian location for the proposed hybrid Si/SiC power module at CL and SL is 42 and 34 years, respectively. Similarly, the CL and SL of conventional Si power modules are 34 and 26 years old, respectively. Reliability improvements of 8 years at both CL and SL were achieved with the proposed Si/SiC power module.

3.2. Reliability-Oriented Performance Evaluation of PV Inverter at the Denmark Location

In this case, the PV inverter's reliability is evaluated using MP data from the Denmark location. A hybrid Si/SiC switch is used in the PV inverter during reliability evaluation, and its effectiveness is analyzed by comparing it with a conventional Si switch.

3.2.1. Calculation of T$_j$

T$_j$ of the proposed hybrid Si/SiC power module and conventional Si power module are calculated for the yearly MP using FETM as shown in Figure 11. From the figure, it is observed that overall, T$_j$ is decreased with the proposed hybrid Si/SiC power module. The maximum and minimum Tj values measured for the proposed hybrid Si/SiC power

module are 90.65 °C and −17.76 °C, respectively, while the conventional Si power module measures 96.37 °C and 17.83 °C.
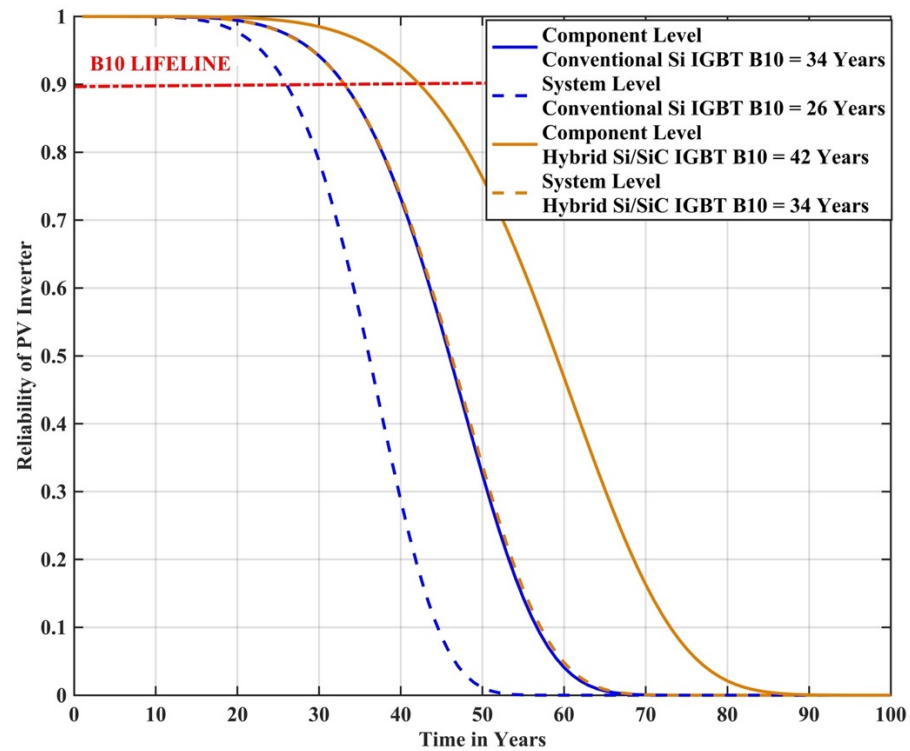

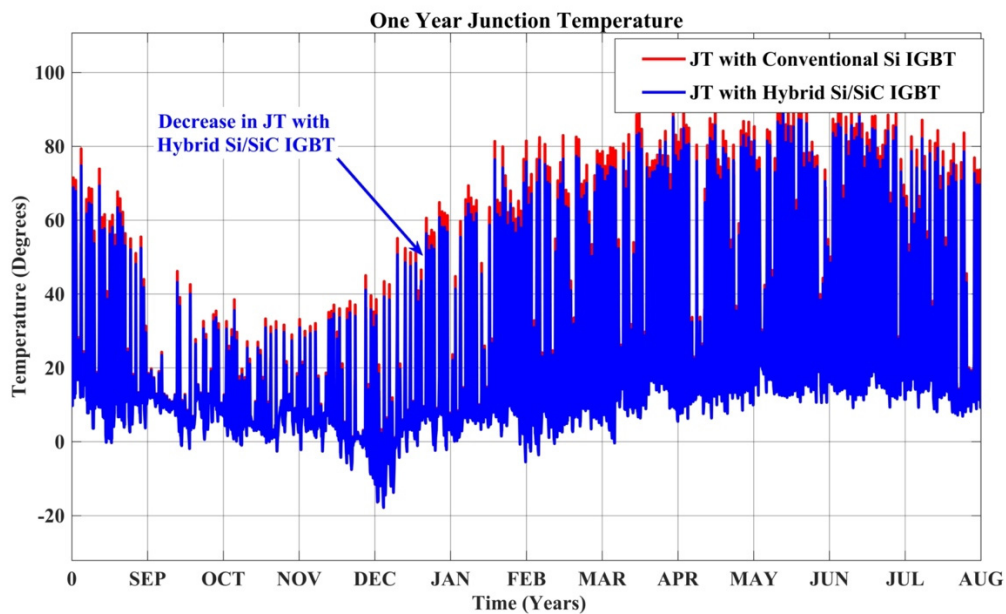**Figure 10.** B_{10} lifetime in India.

Figure 11. Yearly T_j in Denmark.

3.2.2. Rainflow-Counting Algorithm

The T_j variations for the proposed hybrid Si/SiC power module and conventional Si power module are analyzed using the RF algorithm. The parameters N_i, T_{jm}, and ΔT_j, from T_j are obtained using a rainflow-counting algorithm.

The T_j variations histogram, i.e., N_i, T_{jm}, and ΔT for the proposed hybrid Si/SiC power module and conventional Si power module, are plotted in Figure 12. The T_{jm}, i.e., 16.37 °C,

is recorded for the hybrid Si/SiC power module; similarly, 15.91 °C is recorded for the conventional Si power module, as shown in Figure 13.
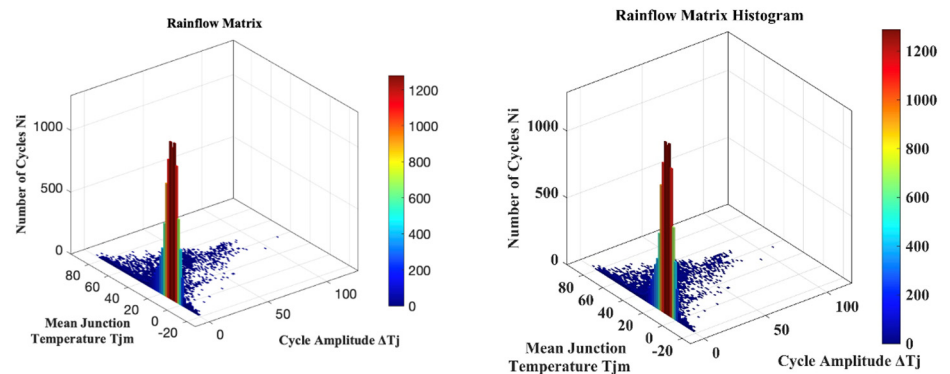
Rainflow Matrix with Conventional IGBT   Rainflow Matrix with Hybrid IGBT
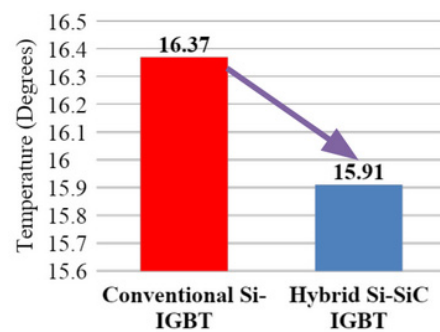
Figure 12. RF matrix in Denmark.

Figure 13. Mean T_j Comparison.

T_{jm} of 0.46 °C is lower with the proposed hybrid Si/SiC power module.

3.2.3. MCS Based B10 Lifetime Evaluation

In this paper, Monte Carlo simulation is used to generate 10,000 samples with 5% variation, and LT is calculated at each sample using Equation (2). All the generated lifetimes are distributed in the Weibull distribution to obtain the reliability function, as shown in Figure 14.

The reliability of the PV inverter is evaluated for the proposed hybrid Si/SiC power module and the conventional Si power module at the CL and SL using Equations (4) and (5), and the B10 lifetime is calculated using Equation (6) as shown in Figure 15. For conventional Si IGBT, the scale parameter $\propto$ is 97.50 and the shape parameter γ is 5.89. Similarly, for hybrid Si/SiC-IGBT scale parameter $\propto$ is 134.14 and the shape parameter γ is 6.19.

The B_{10} lifetime at the Denmark location for the proposed hybrid Si/SiC power module at the CL and the SL is 93 and 74 years, respectively. Similarly, the CL and SL of conventional Si power modules are 67 and 53 years old, respectively. Reliability improvements of 26 years at the CL and 21 years at the SL were achieved with the proposed Si/SiC power module.
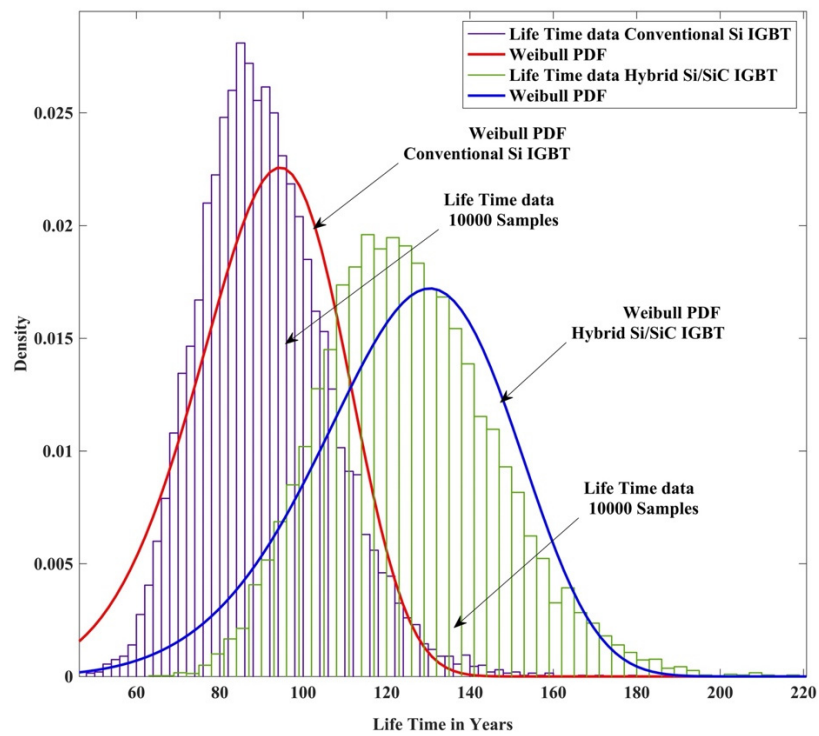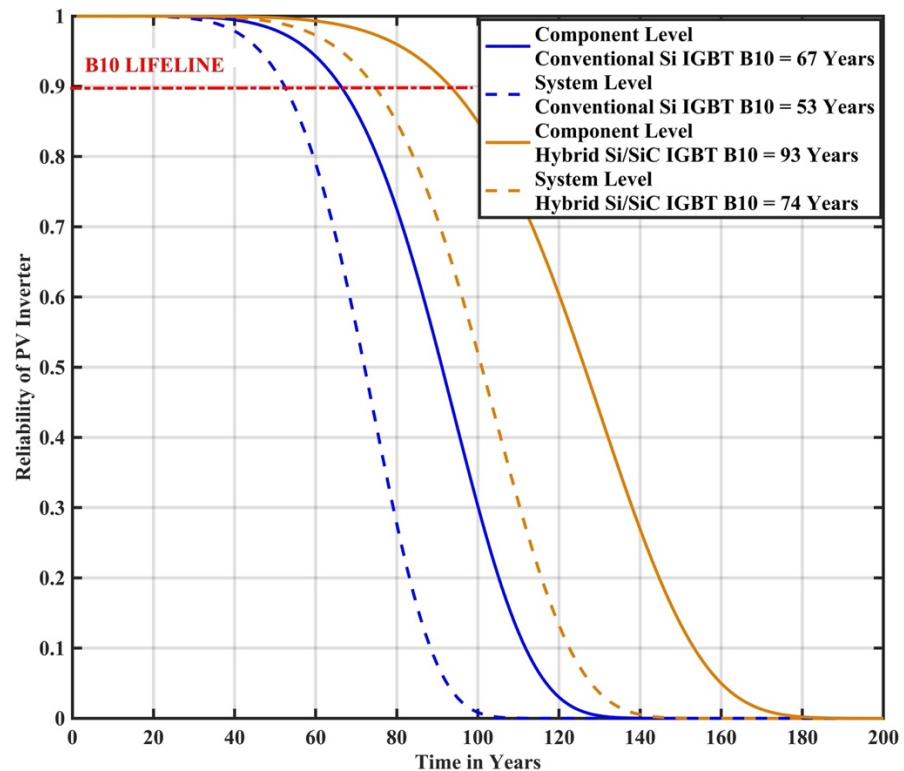
Figure 14. Lifetime distribution.

Figure 15. B_{10} lifetime in Denmark.

3.3. B_{10} Lifetime Comparison

Reliability evaluation of a PV inverter at the India and Denmark locations are performed considering the proposed hybrid Si/SiC power module and conventional Si power module. A B_{10} lifetime is calculated in both cases, and comparative analyses at the CL and SL are shown in Figure 16. At both locations, the B_{10} lifetime of the PV inverter records

the highest value with the proposed hybrid Si/SiC power module in comparison with a conventional Si power module, and hence the reliability performance of a PV inverter is improved. A reliability improvement of 8 years at the CL and the SL was achieved at the Indian location. Similarly, a reliability improvement of 26 years at the CL and 21 years at the SL was achieved with the proposed Si/SiC power module. The cost comparison of conventional Si-IGBT and hybrid Si/SiC-IGBT is presented in Table 2.
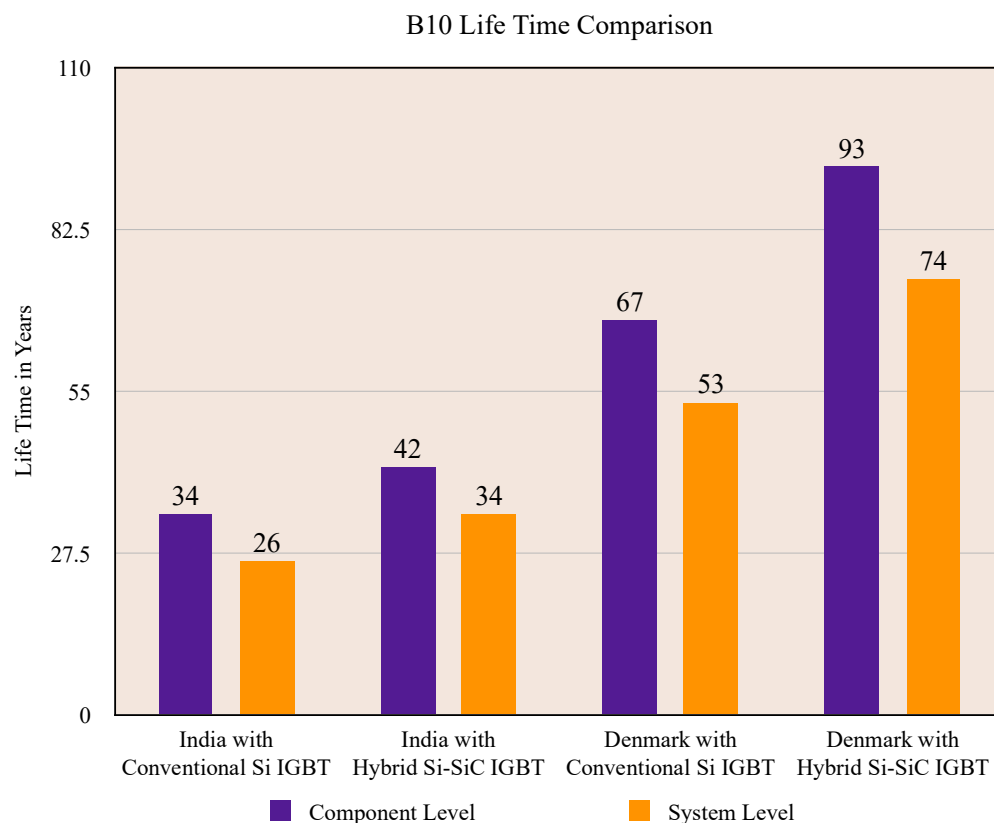

Figure 16. B10 lifetime comparison chart.

Table 2. Cost comparison.

Conventional Si-IGBT (In INR)	Hybrid Si/SiC-IGBT (In INR)
237.02	1095.28

4. Conclusions

This paper presents the reliability evaluation of a PV inverter at the India and Denmark locations, considering a hybrid Si/SiC power module in comparison with a conventional Si power module. A test case of a 3 kW PV inverter for a grid-connected application is considered for reliability analysis. Annual MP (AT, SI) at the India and Denmark locations is considered for this study. T_j at both locations is calculated with the proposed hybrid Si/SiC power module, and its effectiveness is evaluated by comparing it with the conventional Si power module. T_j variations are analyzed using a rainflow-counting algorithm. A hybrid Si/SiC power module records a lower mean T_j than a conventional Si power module. The MC simulation is used to generate 10,000 populations with 5% variation, and LT is calculated at each sample. All samples are fitted into the Weibull distribution. B10 lifetime is calculated at both locations, proposed hybrid Si/SiC power module records the highest value in comparison with the conventional Si power module, and hence the reliability performance of the PV inverter is improved. The current limitation and future step of this work is experimental validation.

Institutional Review Board Statement: Not applicable.

Informed Consent Statement: Not applicable.

Data Availability Statement: Not applicable.

Conflicts of Interest: The authors declare no conflict of interest.

Abbreviations and Nomenclature

PV	Photo Voltaic
Si	Silicon
SiC	Silicon Carbide
IGBT	Insulated gate bipolar transistor
MP	Mission Profile
AT	Ambient Temperature
SI	Solar Irradiance
T_j	Junction Temperature
FETM	Foster Electro-Thermal Model
$Z_{th(j-c)}$	Impedance between junction and case
P_T	Total losses of power
T_c	Temperature of case
N_i	No. of Cycles
T_{jm}	Mean Junction Temperature
ΔT_j	Cycle Amplitude
MCS	Monte Carlo Simulation
CL	Component Level
SL	System Level
RF	Rain Flow

References

1. Busca, C.; Teodorescu, R.; Blaabjerg, F.; Munk-Nielsen, S.; Helle, L.; Abeyasekera, T.; Rodríguez, P. An overview of the reliability prediction related aspects of high power IGBTs in wind power applications. *Microelectron. Reliab.* **2011**, *51*, 1903–1907. [CrossRef]
2. Yang, S.; Bryant, A.; Mawby, P.; Xiang, D.; Ran, L.; Tavner, P. An industry-based survey of reliability in power electronic converters. *IEEE Trans. Ind. Appl.* **2011**, *47*, 1441–1451. [CrossRef]
3. Wang, H.; Liserre, M.; Blaabjerg, F.; de Place Rimmen, P.; Jacobsen, J.B.; Kvisgaard, T.; Landkildehus, J. Transitioning to physics-of-failure as a reliability driver in power electronics. *IEEE J. Emerg. Sel. Top. Power Electron.* **2014**, *2*, 97–114. [CrossRef]
4. Amber, L.; Haddad, K. Hybrid Si IGBT-SiC Schottky diode modules for medium to high power applications. In Proceedings of the IEEE Applied Power Electronics Conference and Exposition (APEC), Tampa, FL, USA, 26–30 March 2017; pp. 3027–3032. [CrossRef]
5. Feng, Z.; Zhang, X.; Wang, J.; Yu, S. A high-efficiency three-level ANPC inverter based on hybrid SiC and Si devices. *Energies* **2020**, *13*, 1159. [CrossRef]
6. Zhang, D.; He, J.; Pan, D. A Megawatt-Scale Medium-Voltage High-Efficiency High Power Density 'SiC + Si' Hybrid Three-Level Propulsion Systems. *IEEE Trans. Ind. Appl.* **2019**, *55*, 5971–5980. [CrossRef]
7. Peng, Z.; Wang, J.; Liu, Z.; Li, Z.; Wang, D.; Dai, Y.; Zeng, G.; Shen, Z.J. Adaptive Gate Delay-Time Control of Si/SiC Hybrid Switch for Efficiency Improvement in Inverters. *IEEE Trans. Power Electron.* **2021**, *36*, 3437–3449. [CrossRef]
8. Ning, P.; Li, L.; Wen, X.; Cao, H. A hybrid Si IGBT and SiC MOSFET module development. *CES Trans. Electr. Mach. Syst.* **2020**, *1*, 360–366. [CrossRef]
9. Mishima, T. A Time-Sharing Current-Fed ZCS High-Frequency Inverter-Based Resonant DC-DC Converter with Si-IGBT/SiC-SBD Hybrid Module for Inductive Power Transfer Applications. *IEEE J. Emerg. Sel. Top. Power Electron.* **2020**, *8*, 506–516. [CrossRef]
10. Han, D.; Noppakunkajorn, J.; Sarlioglu, B. Comprehensive efficiency, weight, and volume comparison of SiC- and Si-based bidirectional dc-dc converters for hybrid electric vehicles. *IEEE Trans. Veh. Technol.* **2014**, *63*, 3001–3010. [CrossRef]

11. Saito, K.; Miyoshi, T.; Kawase, D.; Hayakawa, S.; Masuda, T.; Sasajima, Y. Simplified Model Analysis of Self-Excited Oscillation and Its Suppression in a High-Voltage Common Package for Si-IGBT and SiC-MOS. *IEEE Trans. Electron Devices* **2018**, *65*, 1063–1071. [CrossRef]

12. Peng, Z.; Wang, J.; Liu, Z.; Li, Z.; Dai, Y.; Zeng, G.; Shen, Z.J. A Variable-frequency current-dependent switching strategy to improve tradeoff between efficiency and sic mosfet overcurrent stress in si/sic-hybrid-switch-based inverters. *IEEE Trans. Power Electron.* **2021**, *36*, 4877–4886. [CrossRef]

13. Li, Z.; Wang, J.; Deng, L.; He, Z.; Yang, X.; Ji, B.; Shen, Z.J. Active Gate Delay Time Control of Si/SiC Hybrid Switch for Tj Balance over a Wide Power Range. *IEEE Trans. Power Electron.* **2020**, *35*, 5354–5365. [CrossRef]

14. Guan, Q.X.; Li, C.; Zhang, Y.; Wang, S.; Xu, D.D.; Li, W.; Ma, H. An Extremely High Efficient Three-Level Active Neutral-Point-Clamped Converter Comprising SiC and Si Hybrid Power Stages. *IEEE Trans. Power Electron.* **2018**, *33*, 8341–8352. [CrossRef]

15. Li, D.; Li, X.; Chang, G.; Qi, F.; Packwood, M.; Pottage, D.; Wang, Y.; Luo, H.; Dai, X.; Liu, G. Characterization of a 3.3-kV Si-SiC Hybrid Power Module in Half-Bridge Topology for Traction Inverter Application. *IEEE Trans. Power Electron.* **2020**, *35*, 13429–13440. [CrossRef]

16. Feng, Z.; Zhang, X.; Yu, S.; Zhuang, J. Comparative Study of 2Si&C4Si Hybrid Configuration Schemes in ANPC Inverter. *IEEE Access* **2020**, *8*, 33934–33943. [CrossRef]

17. Wang, J.; Li, Z.; Jiang, X.; Zeng, C.; Shen, Z.J. Gate Control Optimization of Si/SiC Hybrid Switch for Tj Balance and Power Loss Reduction. *IEEE Trans. Power Electron.* **2019**, *34*, 1744–1754. [CrossRef]

18. Li, Z.; Wang, J.; He, Z.; Yu, J.; Dai, Y.; Shen, Z.J. Performance Comparison of Two Hybrid Si/SiC Device Concepts. *IEEE J. Emerg. Sel. Top. Power Electron.* **2020**, *8*, 42–53. [CrossRef]

19. Li, Z.; Wang, J.; Ji, B.; Shen, Z.J. Power loss model and device sizing optimization of Si/SiC hybrid switches. *IEEE Trans. Power Electron.* **2020**, *35*, 8512–8523. [CrossRef]

20. Ning, P.; Yuan, T.; Kang, Y.; Han, C.; Li, L. Review of Si IGBT and SiC MOSFET based on hybrid switch. *Chin. J. Electr. Eng.* **2019**, *5*, 20–29. [CrossRef]

21. Song, X.; Zhang, L.; Huang, A.Q. Three-Terminal Si/SiC Hybrid Switch. *IEEE Trans. Power Electron.* **2020**, *35*, 8867–8871. [CrossRef]

22. Noppakunkajorn, J.; Han, D.; Sarlioglu, B. Analysis of High-Speed PCB with SiC Devices by Investigating Turn-Off Overvoltage and Interconnection Inductance Influence. *IEEE Trans. Transp. Electrif.* **2015**, *1*, 118–125. [CrossRef]

23. Naderi, E.; Bibek, K.C.; Ansari, M.; Asrari, A. Experimental Validation of a Hybrid Storage Framework to Cope With Fluctuating Power of Hybrid Renewable Energy-Based Systems. *IEEE Trans. Energy Convers.* **2021**, *36*, 1991–2001. [CrossRef]

24. Naderi, E.; Asrari, A. Experimental Validation of Grid-Tied and Standalone Inverters on a Lab-scale Wind-PV Microgrid. In Proceedings of the 2021 IEEE International Power and Renewable Energy Conference (IPRECON), Kollam, India, 24–26 September 2021; pp. 1–6. [CrossRef]

25. Kshatri, S.S.; Dhillon, J.; Mishra, S. Reliability evaluation of grid connected pv inverter considering panel degradation rate and oversizing at Indian location. *J. Crit. Rev.* **2020**, *7*, 1710–1714.

26. Global Modeling and Assimilation Office (GMAO). MERRA-2 tavg1_2d_slv_Nx: 2d,1-Hourly,Time-Averaged,Single-Level,Assimilation,Single-Level Diagnostics V5.12.4, Greenbelt, MD, USA, Goddard Earth Sciences Data and Information Services Center (GES DISC). 2015. Available online: https://www.soda-pro.com/web-services/meteo-data/merra (accessed on 1 November 2018).

27. Gatla, R.K.; Chen, W.; Zhu, G.; Wang, J.V.; Kshatri, S.S. Lifetime comparison of IGBT modules in Grid-connected Multilevel PV inverters Considering MP. In Proceedings of the 2019 10th International Conference on Power Electronics and ECCE Asia (ICPE 2019—ECCE Asia), Busan, Republic of Korea, 27–30 May 2019.

28. Bayerer, R.; Herrmann, T.; Licht, T.; Lutz, J.; Feller, M. Model for power cycling lifetime of IGBT Modules? Various factors influencing lifetime. In Proceedings of the 5th International Conference on Integrated Power Electronics Systems, Nuremberg, Germany, 11–13 March 2008.